Restoration of images with optical aberrations and quantization in a transform domain

Edmund Y. Lam[a] and Michael K. Ng[b]

[a]Department of Electrical and Electronic Engineering, University of Hong Kong, Hong Kong;
[b]Department of Mathematics, University of Hong Kong, Hong Kong.

ABSTRACT

Digital images generally suffer from two main sources of degradations. The first includes errors introduced in imaging, such as blurring due to optical aberrations and sensor noise. The second includes errors introduced during the processing. One particular example is the quantization noise arising from lossy compression. While image restoration is concerned with the recovery of the object from these degradations, often we only deal with one type of the error at a time. In this paper, we present a restoration algorithm that handles images with optical aberrations and quantization in a transform domain. We show that it can be cast in a joint optimization setting, and demonstrate how it can be solved efficiently through alternating minimization. We also prove analytically that the algorithm is globally convergent to a unique solution when the restoration uses either H^1-norm or TV-norm regularization. Simulation result asserts that this joint minimization produces images with smaller relative errors compared to a standard regularization model.

Keywords: Image restoration, optical aberrations, quantization, discrete cosine transform, joint optimization, alternating minimization

1. INTRODUCTION

In recent years, multimedia communication has become more and more popular in a diverse array of applications. This is in part spawned by the rapid advancement in electronic sensor technology. With either charge coupled devices (CCD) or complementary metal-oxide semiconductor (CMOS) imagers, the number of pixels that can be found in digital still and video cameras have increased substantially. Larger images require a wider bandwidth for transmissions. In most cases, they need to be subjected to a lossy compressor for effective communication and storage.

Lossy compression is usually achieved by quantization of the image in a transformed domain. In JPEG, the image undergoes block-based discrete cosine transform (DCT) before the DCT coefficients are quantized according to a pre-defined quantization matrix.[1] In JPEG 2000, the transform basis is changed to wavelets, and quantization is performed on the wavelet coefficients at the different subbands.[2] Similar techniques are used for many other image and video compression standards.[3] Mathematically, the quantization step can be considered as an addition of quantization noise, whereby the visual appearances of the images remain largely unaffected while the coding of the resulting transformed coefficients becomes much more effective. More often in reality, though, the visual quality of the images is necessarily degraded, and we seek image restoration schemes to remove the degradation as far as possible.

Quantization noise is not the only source of degradation, however. In many imaging settings, there are blurring of the images introduced during the image capture. The most common types are defocusing and motion blur, both of which can be modeled as space-invariant degradations and have been studied extensively in the image restoration literature.[4–6] As the sensor pixel size decreases, some other optical distortions become more apparent. For example, for the first-order Seidel aberrations, we have spherical aberration, coma, astigmatism, curvature of field, as well as barrel and pincushion distortion.[7] Although all except spherical aberration is space-variant, some can be made space-invariant by appropriate geometric coordinate transformations under certain

Further author information: (Send correspondence to Edmund Lam.)
Edmund Lam: E-mail: elam@eee.hku.hk
Michael Ng: E-mail: mng@maths.hku.hk

Computational Imaging II, edited by Charles A. Bouman,
Eric L. Miller, Proc. of SPIE-IS&T Electronic Imaging,
SPIE Vol. 5299 © 2004 SPIE and IS&T · 0277-786X/04/$15

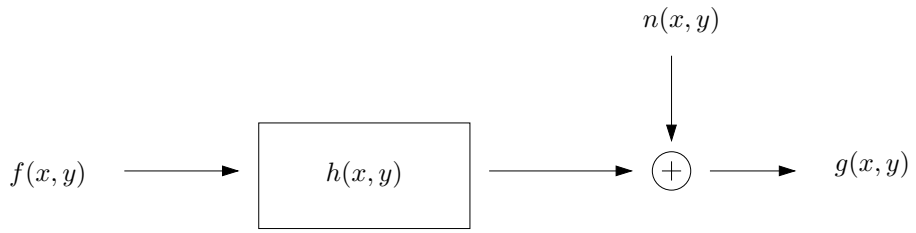

Figure 1. Block diagram for the imaging system.

conditions.[8] Therefore, we restrict ourselves to the restoration of linear space-invariant blurs in this paper for their simplicity in modeling, while bearing in mind the possibilities of extending the algorithm to handle a wider class of degradations.

While both linear space-invariant blur and transformed-domain quantization are acknowledged sources of degradations, most image restoration algorithms deal with them in separate processes. In fact, most image restoration algorithms assume that the quantization noise is small and can be ignored. This assumption may be valid for images with low compression, but when we have severe compression, quantization noise cannot be ignored. In this paper, we propose an image restoration algorithm that directly restores the blurred and quantized image. Note that this is slightly different from restoration schemes designed in the compressed domain, where we seek to embed the restoration along the compression codec to minimize the computational burden.[9,10] These algorithms are suitable for on-camera restorations, where computation capability is limited and compression codec is readily available as part of the imaging pipeline. In contrast, our proposed scheme here is suitable for operation after the images are downloaded to a computer host, where we can afford more computation such as with the use of iterative techniques.

The paper is organized as follows: In section 2, we present a mathematical analysis of the combined effects of linear space-invariant degradation and transform domain quantization. Then, in section 3, the detail of the algorithm is presented, paying attention to its setting, the alternating minimization algorithm, and the special case with symmetric blur. Simulation results will then be presented in section 4, with some concluding remarks to follow.

2. EFFECTS OF QUANTIZATION AND BLUR

For linear space-invariant degradation, the observed image and the original object can be related simply by a convolution relationship. Imaging is modeled with the well-known equation

$$g(x,y) = h(x,y) * f(x,y) + n(x,y), \tag{1}$$

where $g(x,y)$ is the observed image, $f(x,y)$ is the original object, and $h(x,y)$ is the point spread function, which is the inverse Fourier transform of the Optical Transfer Function (OTF). $n(x,y)$ represents noise in the imaging system, which is typically modeled as additive white Gaussian.[11] A block diagram representing the imaging system is shown in Fig. 1. For simplicity in description, we will use an equivalent matrix representation of equation (1) by raster-scanning the images to obtain

$$\mathbf{g} = H\mathbf{f} + \mathbf{n}. \tag{2}$$

Note that H is a block Toeplitz matrix and can be diagonalized by the two-dimensional discrete Fourier transform (DFT) if we use circular convolution in equation (1).

After the image is captured in the imaging system, it undergoes quantization in the transformed domain. We represent the image transform by a matrix operation C^T. This can represent Fourier transform, Cosine transform, or other linear transforms, where C is a unitary matrix. Quantization is computed by a multiplication with a

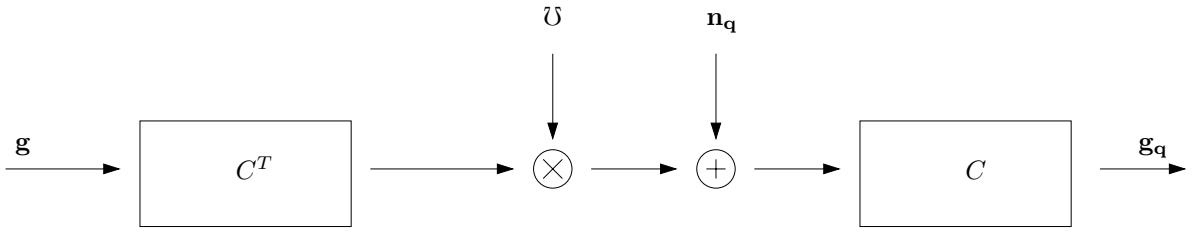

(a) Image compression.

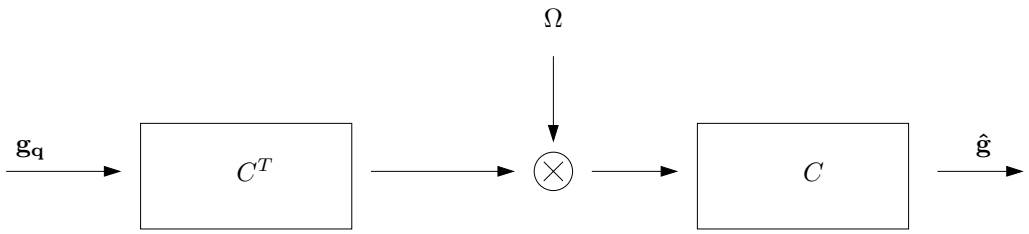

(b) Image decompression.

Figure 2. Block diagrams for compression and decompression.

diagonal matrix $\mathcal{U}$ that scales the quantized coefficients, and an addition of quantization noise $\mathbf{n_q}$. Conceptually, the quantized image can be multiplied by C to bring it back to the spatial domain,

$$\mathbf{g_q} = C\mathcal{U}C^T\mathbf{g} + C\mathbf{n_q}, \tag{3}$$

where $\mathbf{g_q}$ is the quantized image, although often in practice it remains in the transformed domain and the quantized coefficients are losslessly encoded for transmission or storage.

In decoding, we compute

$$\begin{aligned} \hat{\mathbf{g}} &= C\Omega C^T\mathbf{g_q} \\ &= C\Omega\mathcal{U}C^T\mathbf{g} + C\Omega\mathbf{n_q} \\ &= C\Omega\mathcal{U}C^TH\mathbf{f} + C\Omega\left(\mathcal{U}C^T\mathbf{n} + \mathbf{n_q}\right), \end{aligned} \tag{4}$$

where $\hat{\mathbf{g}}$ is the decompressed image and Ω is a diagonal matrix that scales the quantized coefficients. The block diagrams for compression and decompression are shown in Fig. 2(a) and (b) respectively.

Ideally, $\hat{\mathbf{g}}$ should be close to $H\mathbf{f}$. Therefore, we can perform simultaneous dequantization and restoration by minimizing the following expression

$$\begin{aligned} \left(\tilde{\mathbf{f}}, \tilde{\Omega}\right) &= \arg\min_{\mathbf{f},\Omega} \|\hat{\mathbf{g}} - H\mathbf{f}\| \\ &= \arg\min_{\mathbf{f},\Omega} \|C\Omega C^T\mathbf{g_q} - H\mathbf{f}\| \\ &= \arg\min_{\mathbf{f},\Omega} \|C\Omega\mathcal{U}C^TH\mathbf{f} + C\Omega\left(\mathcal{U}C^T\mathbf{n} + \mathbf{n_q}\right) - H\mathbf{f}\| \\ &= \arg\min_{\mathbf{f},\Omega} \| \left(C\Omega\mathcal{U}C^T - I\right)H\mathbf{f} + C\Omega\left(\mathcal{U}C^T\mathbf{n} + \mathbf{n_q}\right) \|. \end{aligned} \tag{5}$$

Note that if $\mathbf{n_q}$ is small, the above expression can be simplified to a linear least-square restoration where the solution is readily obtained by Wiener filtering.[12] However, for high compression ratio, $\mathbf{n_q}$ is non-negligible and it alters the noise spectrum in a complex manner if we attempt to use the Wiener filter. Instead, in the next section, we propose an iterative technique using alternating minization to compute the restoration.

3. IMAGE RESTORATION ALGORITHM

3.1. Algorithm Setting

It is well-known that image restoration with equation (5) is an ill-posed problem and regularization is necessary for a stable solution. Therefore, we actually tackle the modified problem

$$\min_{\mathbf{f},\Omega} J \quad \equiv \quad \frac{1}{2}\|H\mathbf{f} - C\Omega C^T\mathbf{g_q}\|_2^2 + \alpha R(\mathbf{f}). \tag{6}$$

α is a positive parameter which measures the trade-off between a good fit and the regularity of the solution $\mathbf{f}$. In the model, the H^1-norm regularization functional can be applied to $R(\mathbf{f})$ in equation (6). However, the H^1-norm regularization functional tends to attenuate the high frequency information of $\mathbf{f}$. We can also use the total variation (TV) regularization functional.[13] We remark that TV-norm allows the discontinuities in $\mathbf{f}$, thus making it superior to the H^1 regularization in cases where $\mathbf{f}$ can have discontinuities, such as with edges.

3.2. Alternating Minimization

In this subsection, we consider the alternating minimization algorithm to solve the joint minimization model in (6). With an initial guess $\mathbf{f}^0$ for $\mathbf{f}$, we minimize equation (6) by first solving $\Omega^0 = \arg\min_{\Omega} J(\mathbf{f}, \Omega)$ and then $\mathbf{f}^1 = \arg\min_{\mathbf{f}} J(f, \Omega^0)$. The algorithm is given as follows:

Alternating Minimization Algorithm:

Given $\mathbf{f}^0$: iterating $k = 0, 1, 2, \ldots$, until convergence
Step (i) Solve $\Omega^k = \arg\min_{\Omega} \ J(\mathbf{f}^k, \Omega)$
Step (ii) Solve $\mathbf{f}^{k+1} = \arg\min_{\mathbf{f}} \ J(\mathbf{f}, \Omega^k)$

In Step (i) of the alternating minimization algorithm, the diagonal matrix $\Omega^k = \arg\min_{\Omega} \ J(\mathbf{f}^k, \Omega)$ can be determined by solving the corresponding Euler-Lagrange equation:

$$\nabla_\Omega J = \Omega C^T\mathbf{g_q} - C^T H\mathbf{f} = 0. \tag{7}$$

Similarly, in Step (ii), the image $\mathbf{f}^{k+1} = \arg\min_{\mathbf{f}} \ J(\mathbf{f}, \Omega^k)$ can be found by solving the equation:

$$\nabla_{\mathbf{f}} J = H^T H\mathbf{f} + \alpha r(\mathbf{f}) - H^T C\Omega C^T\mathbf{g_q} = 0. \tag{8}$$

We remark that if $R(\mathbf{f})$ is the H^1-norm regularization functional, then

$$r(\mathbf{f}) = -\triangle\mathbf{f}, \tag{9}$$

where $\triangle$ denotes the Laplacian operator with the Neumann boundary condition. The discrete version of $-\triangle\mathbf{f}$ is the discrete 2-dimensional Laplacian matrix L with the Neumann boundary condition. Note that the matrix L can be diagonalized by the discrete cosine transform matrix, see for instance Ref. 14. If $R(\mathbf{f})$ is the total-variation regularization functional, then

$$r(\mathbf{f}) = -\nabla \cdot \left(\frac{\nabla\mathbf{f}}{|\nabla\mathbf{f}|}\right). \tag{10}$$

Due to the term $1/|\nabla\mathbf{f}|$, $r(\mathbf{f})$ is a degenerate nonlinear second order diffusion term. The degeneracy can be removed by modifying the diffusion coefficient by considering

$$r(\mathbf{f}) = -\nabla \cdot \left(\frac{\nabla\mathbf{f}}{\sqrt{|\nabla\mathbf{f}|^2 + \beta}}\right) \tag{11}$$

for a small value of β.

3.3. Analysis of Algorithm

We can use alternating minimization algorithm to find the minimizer. To show the convergence of the alternating minimization algorithm, we first establish the following two lemmas.

LEMMA 3.1. *The Hessian $Hess(J)$ is positive definite under H^1-norm regularization functional.*

Proof. By direct computation, the Hessian $Hess(J)$ is given by

$$Hess(J) = \begin{pmatrix} H^T H + \alpha L & -H^T C G \\ -G^T C^T H & G^T G \end{pmatrix}, \tag{12}$$

where $G = \text{diag}(C^T \mathbf{g_q})$ and $\text{diag}(\mathbf{x})$ denotes a diagonal matrix whose diagonal is given by the vector $\mathbf{x}$. We can show that it is positive definite.

LEMMA 3.2. *The Hessian $Hess(J)$ is positive definite under TV-norm regularization functional.*

Proof. The proof is similar.

With these two lemmas, we have the following main theorem.

THEOREM 3.3. *For any initial guess $\mathbf{f}^0$, the alternating minimization algorithm converges globally to a unique solution under H^1-norm or TV-norm regularization.*

Proof. The alternating minimization algorithm can be stated as a block coordinate descent method on $\mathbf{f}$ and Ω. Since $Hess(J)$ is positive definite, J is strictly convex on $\mathbf{f}$ and Ω. By using Proposition 2.7.1 of Ref. 15, the alternating minimization algorithm is globally convergent toward the unique global minimizer.

3.4. Symmetric Blur

For symmetric blurring operators, H can be diagonalized by the discrete cosine transform operator C, i.e., $H = C\Lambda C^T$,[14] where Λ is a diagonal matrix. Also when using the H^1-norm regularization functional, L can be diagonalized by C as well, i.e., $L = C\Phi C^T$,[14] where Φ is a diagonal matrix. In this situation, the minimization problem becomes

$$\min_{f,\Omega} J = \frac{1}{2}\|\Lambda C^T \mathbf{f} - \Omega C^T \mathbf{g_q}\|_2 + \alpha \mathbf{f}^T L \mathbf{f}. \tag{13}$$

In Step (i), we solve

$$\nabla_\Omega J = \Omega C^T \mathbf{g_q} - \Lambda C^T \mathbf{f} = 0, \tag{14}$$

the diagonal part of Ω is equal to $C^T \mathbf{g_q} \odot \Lambda C^T \mathbf{f}$, where $\odot$ denotes pointwise division. Similarly, in Step (ii),

$$\nabla_{\mathbf{f}} J = (\Lambda^T \Lambda + \alpha\Phi) C^T \mathbf{f} - \Lambda^T \Omega C^T \mathbf{g_q} = 0, \tag{15}$$

i.e., the restored image $\mathbf{f}$ is equal to $C(\Lambda^T \Omega C^T \mathbf{g_q} \odot \Lambda^T \Lambda + \alpha + \Phi)$.

4. SIMULATIONS

In this section, we illustrate the effectiveness of using the new minimization model and the efficiency of the alternating minimizing algorithm. The simulation results are shown in Figs. 3 and 4.

In each Figure, we begin with a sharp original image ("mri" image). Gaussian white noise n with

$$\frac{\|Hf\|_2}{\|n\|_2} = 5 \tag{16}$$

is added to the frequency domain of the blurred images. In the test, the stopping criterion of the alternating minimization algorithm is $||\mathbf{f}^{(k)} - \mathbf{f}^{(k-1)}||_2 < 10^{-3}$, where $f^{(k)}$ is the kth iterate of the algorithm.

α	without blur	the blur $[1/3, 1/3, 1/3] \otimes [1/3, 1/3, 1/3]$
0.0001	39	2
0.001	37	37
0.01	70	100
0.1	120	121

Table 1. Number of the iterations required for different regularization parameters.

Figures 3 and 4 show the restored images using the standard model

$$\min_{\mathbf{f}} \tilde{J} \equiv \frac{1}{2}\|H\mathbf{f} - \mathbf{g_q}\|_2^2 + \tilde{\alpha}R(\mathbf{f}) \tag{17}$$

and our proposed model in equation (6). Here the optimal regularization parameters $\tilde{\alpha}$ and α are suitably chosen so that they minimize the relative error of the reconstructed image to the original image:

$$\frac{||\mathbf{f}_{restored} - \mathbf{f}_{original}||}{||\mathbf{f}_{original}||}$$

where $\mathbf{f}_{restored}$ is the restored image by the algorithm and $\mathbf{f}_{original}$ is the original image. The same procedure is applied to the two models. In Figures 3 and 4, the regularization parameters $\tilde{\alpha}$ and α are 0.25 and 0.001 respectively. Moreover, their corresponding relative errors are reported in their captions. We find that the relative errors of the restored images using joint minimization model is less than that of restored image using the model in equation (17). We see that our proposed model gives slightly better restored image.

In Table 1, we show the number of iterations of the alternating minimizing algorithm required for different values of α. In the tests, we use the blurred and noisy image as the initial guess for the joint minimization model. We see from Table 1 that when α increases, the number of iterations required for convergence increases.

5. CONCLUSIONS

In this paper we present an algorithm that can restore images with optical aberrations and quantization in a transform domain. Using an alternating minimization approach, we first assert its global convergence behavior mathematically and then observe its ability to restore images with simulation. Together they suggest that this approach is viable to give images with somewhat better quality than if we use a standard restoration technique that targets the deblurring alone.

REFERENCES

1. W. Pennebaker and J. Mitchell, *JPEG Still Image Data Compression Standard*, Van Nostrand Reinhold, New York, 1992.
2. D. Taubman and M. Marcellin, *JPEG 2000: Image Compression Fundamentals, Standards and Practice*, Kluwer Academic Publishers, Boston, 2001.
3. B. G. Haskell, P. G. Howard, Y. A. LeCun, A. Puri, J. Ostermann, M. R. Civanlar, L. Rabiner, L. Bottou, and P. Haffner, "Image and video coding — emerging standards and beyond," *IEEE Transactions on Circuit and Systems for Video Technology* **8**, pp. 814–37, November 1998.
4. H. Andrews and B. Hunt, *Digital Image Restoration*, Prentice Hall, Englewood Cliffs, New Jersey, 1977.
5. A. K. Katsaggelos, *Digital Image Restoration*, Springer-Verlag, New York, 1991.
6. M. R. Banham and A. K. Katsaggelos, "Digital image restoration," *IEEE Signal Processing Magazine* **14**, pp. 24–41, March 1997.
7. W. Smith, *Modern Optical Engineering*, McGraw-Hill, New York, 2000.
8. A. Sawchuk and M. Peyrovian, "Restoration of astigmatism and curvature of field," *Journal of the Optical Society of America* **65**, pp. 712–715, June 1975.

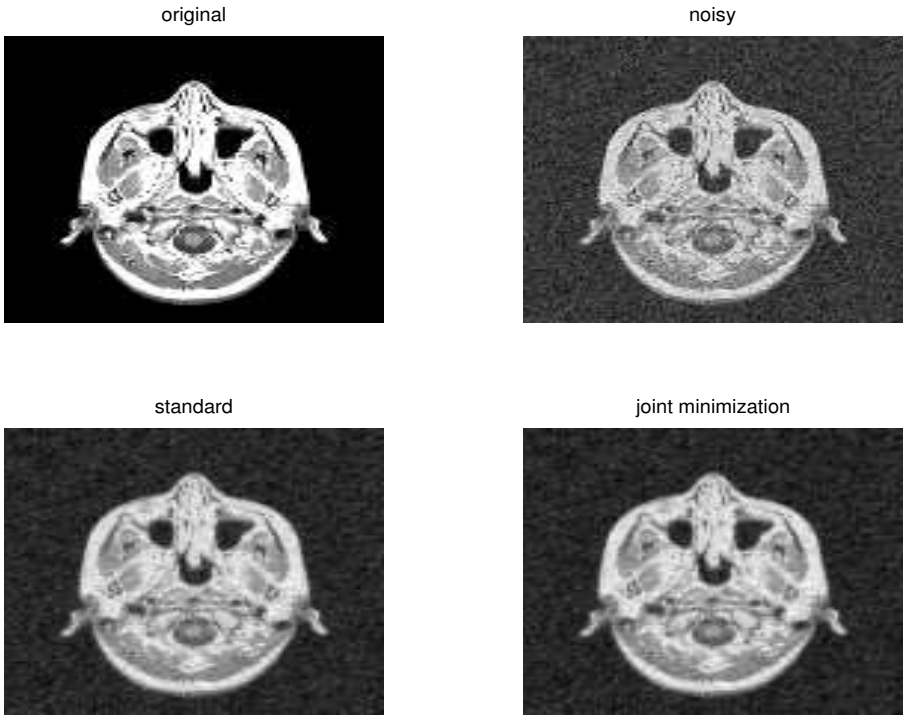

Figure 3. Restored images without blur. The relative errors from the standard restoration and the joint minization restoration methods are 0.1535 and 0.1527 respectively.

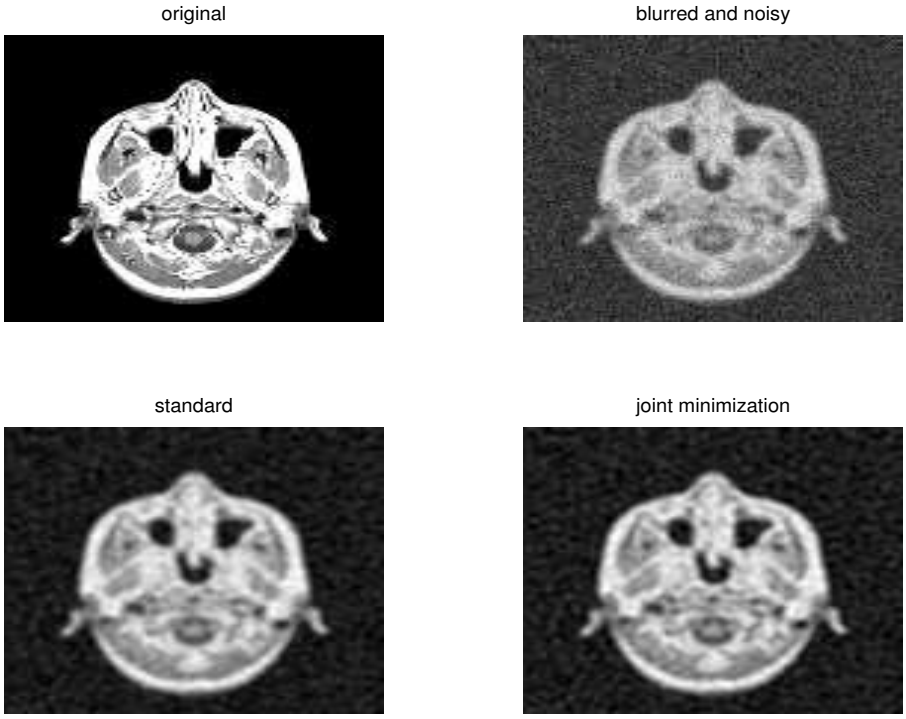

Figure 4. Restored images with the bluring $[1/3, 1/3, 1/3] \otimes [1/3, 1/3, 1/3]$. The relative errors from the standard restoration and the joint minization restoration methods are 0.2121 and 0.2097 respectively.

9. E. Y. Lam and J. W. Goodman, "Discrete cosine transform domain restoration of defocused images," *Applied Optics* **37**, pp. 6213–6218, September 1998.
10. E. Y. Lam, "Digital restoration of defocused images in the wavelet domain," *Applied Optics* **41**, pp. 4806–4811, August 2002.
11. E. Y. Lam, "Image restoration in digital photography," *IEEE Transactions on Consumer Electronics* **49**, pp. 269–274, May 2003.
12. J. W. Goodman, *Introduction to Fourier Optics*, McGraw-Hill, New York, second ed., 1996.
13. L. Rudin, S. Osher, and E. Fatemi, "Nonlinear total variation based noise removal algorithms," *Physica D* **60**, pp. 259–268, 1992.
14. M. Ng, R. Chan, and W. Tang, "A fast algorithm for deblurring models with neumann boundary conditions," *SIAM Journal of Scientific Computing* **21**, pp. 851–866, 1999.
15. D. P. Bertsekas, *Nonlinear Programming*, Athena, Belmont, MA, 1995.